Multi-Scale Modeling of Magnetostrictive Materials

Olivier Hubert, Laurent Daniel, Laurent Bernard

Chapter 1

Multi-scale modelling of magnetostrictive materials

Olivier Hubert [a] , Laurent Daniel [b] , and Laurent Bernard [c]

[a] *LMT (ENS Paris-Saclay, CNRS, Université Paris-Saclay) 61 avenue du président Wilson, 94235 Cachan Cedex - France*

, [b] *GeePs | Group of electrical engineering - Paris (UMR CNRS 8507, CentraleSupélec, Univ. Paris-Sud, Université Paris-Saclay, Sorbonne Université) 3 rue Joliot-Curie, Plateau de Moulon 91192 Gif-sur-Yvette Cedex, France*

, [c] *GRUCAD/EEL/CTC, Universidade Federal de Santa Catarina, Florianópolis 88040-900, Brazil*

When a magnetic material is subjected to a magnetic field, it magnetises. When subjected to a mechanical stress, it deforms. As shown by Joule in the early 19th century (1847), the application of a magnetic field can also produce a deformation: this is the magnetostriction phenomenon [1]. Villari showed few years later (1865) that a mechanical stress has also the ability to magnetise a material (more precisely to change its initial magnetisation): in this chapter it will be referred to as piezomagnetism, but it is also called inverse magnetostriction or Villari effect. These two phenomena derive from the same coupling: the magnetoelastic coupling [2]. A material is called *magnetostrictive material* if it exhibits this coupling and if this coupling is then used for an application. An accurate modelling of the constitutive behaviour of magnetostrictive materials involves consequently an accurate description of magneto-mechanical effects.

This chapter begins by a short introduction where magnetomechanical coupling consequences and applications are discussed. Multiscale modelling is then presented, preceded by a section devoted to the thermodynamics of magneto-mechanical coupling, and followed by some illustrations showing the ability of such approach to model complex behaviour. A final discussion is proposed where some current research areas are presented.

This chapter is on the other hand correlated to the chapter "Multi-scale modelling of magnetic materials" since the magneto-elastic coupling is the main coupling addressed in this previous chapter. The present chapter proposes a thermodynamic approach giving a formal framework for the admissibility of conservative and dissipative forms of constitutive magneto-elastic laws. We focus here on the magnetostrictive behaviour and examples will deal mainly with this aspect. Note that simplification procedures and numerical implementation strategies are not discussed. They are addressed in the chapter "Multi-scale

modelling of magnetic materials".

1.1 MAGNETOMECHANICAL COUPLING CONSEQUENCES AND APPLICATIONS

1.1.1 Influence of stress on magnetic behaviour

In most practical electromagnetic applications, magnetic materials are subjected to stress inherited from forming process or appearing in use. As examples, inertial stresses in high rotational speed systems for aeronautic equipments, stresses due to binding process (encapsulation) of electrical machines and actuators, residual stress associated to plastic straining (forming) or cutting process can be mentioned. A change of the mechanical state in a magnetostrictive material (including the wide family of ferritic steels) will produce a change of the magnetic behaviour (e.g. magnetic permeability, magnetic losses). Mechanical stress must consequently be taken into account in the design of electromagnetic systems (size, choice of appropriate materials, thermal treatments) in order to avoid misdesign issues. The question is of particular importance in the field of material optimisation for magnetic transformers and rotating machines.

1.1.2 Magnetomechanical sensors - Piezomagnetic behaviour

Villari effect can be used for sensors (force, torque) or non-destructive evaluation (NDE) applications since the variation of magnetisation can give an information about the mechanical state. Sensors based on magnetomechanical behaviour must exhibit a large coupling. Specifically, the variation of the magnetisation with respect to the applied stress should be high for an appropriate sensitivity. Rare earth elements (Tb, Dy) are often used as secondary elements in alloys that are employed as magnetic sensors, because they exceptionally enhance the magnetomechanical properties of these materials. For example, Terfenol D exhibits very high magnetostriction coefficients, typically 1000 ppm at room temperature and a coupling factor of about 1 kA/m/MPa. Magneto-elastic coupling can also be used in NDE for the detection of residual stresses in ferromagnetic materials. The available techniques are usually based on the measurement of hysteresis loops, incremental permeability, eddy currents, Barkhausen noise or a mix of these techniques. Some issues are related on the one hand to the low levels of magnetostriction of the considered materials (thus a low sensitivity to mechanical stress) and to the generally non-linear (or even non-monotonic) character of this sensitivity on the other hand.

1.1.3 Actuators

Magnetic actuators are discussed in a dedicated chapter ("Magnetostrictive actuators"). Magnetostrictive actuators use the complementary part of the coupling:

deformation during magnetisation. They are usually (but not necessarily) made of solid magnetostrictive materials wounded by a coil (current-driven sensors) or indirectly magnetised by a permanent magnet. The smart materials used for these applications are usually giant magnetostrictive materials. Among them, Terfenol and Galfenol are probably the most popular, allowing a good ratio between deformation and power supply (requiring however magnetic field of the order of 100kA/m). Magneto-rheologic materials can also be used as actuators with deformations of the order of 0.1%. Magnetic Shape Memory Materials are another option for magnetic driven actuators. The intrinsic magnetostriction of these materials is large (about 100ppm) but insufficient for actuator application. Their deformation comes from martensite reorientation (or twinning). A strain higher than 5% can be reached. Their sensitivity to stress is the main obstacle to their applications as actuators. Stress results sometimes in a dramatic reduction of the amplitudes of deformation that the system can develop. Multiscale modelling can be a key to better understand this phenomenon and find adapted implementation solutions.

1.1.4 Vibrations and noise emitted by transformers and electrical machines

High power transformers are made of sets of primary and secondary windings wounded around the legs of the transformer. They are usually made of very soft ferromagnetic materials for high efficiency. The transformer core is made of an assembly of hundreds of thin sheets to limit the eddy current and ensure a homogeneous magnetic field through the thickness. Associated to their forming process (hot/cold rolling, heat treatments), transformer sheets usually exhibit anisotropic magnetic behaviour. Classical on-board electrical transformers are for example made of Non-Oriented FeSi that lead to a high induction at a given magnetic field level along the rolling direction (RD). The use of magnetic materials presenting a high power density (e.g. Iron-Cobalt) is one solution to reduce the mass of these transformers. Prototypes generate unfortunately a loud noise in operation. This noise is caused by the magnetostrictive strain. Multiscale modelling of these materials combined with an appropriate consideration of boundary conditions could help for design optimization and noise decrease.

1.2 THERMODYNAMICS OF MAGNETO-ELASTIC COUPLING

This chapter addresses the multiscale modelling of a representative volume element (RVE), leading to a *local* constitutive (magnetostrictive) behaviour. All developments are made in the framework of continuum mechanics, electromagnetics and thermodynamics [3].

1.2.1 Scales

In the following, g denotes a grain. It is supposed to be composed of several phases ϕ (typically ferrite, austenite, martensite,...), that may be separated in different variants. Phases remain at constant volume fraction in the proposed modelling[1]. α denotes a magnetic domain family inside the considered ferromagnetic phase and represents the lower scale (one *family* indicates a set of domains exhibiting the same easy axis). The scale organization is illustrated in figure 1.1, from the domain scale to the RVE. At each scale, some physical fields can be considered as homogeneous leading to some simplifications in the energy description. A first step consists in building an energy function at the domain scale where anisotropic crystallographic phenomena are significant and some fields can be simplified. At the domain family scale, two main phenomena are considered to contribute to the macroscopic magnetization process, namely domain wall motion (change in volume of the domain family), and magnetisation rotation.

«FIGURE 1 HERE»

1.2.2 First principle, powers and form effect

The first law of thermodynamics is considered at the local scale (domain family scale). Index α is used to underline this local expression. The total mechanical power density p_α is the sum of the time derivatives of the kinetic energy density e^c_α and internal energy density u_α (time derivation is indicated by a dot ($\dot{}$)). It varies under the effect of electromagnetic power p^e_α, mechanical power p^m_α, heat sources q_α and heat transfer $-\mathrm{div}(\mathbf{q}^s_\alpha)$ [4].

$$p_\alpha = \dot{u}_\alpha + \dot{e}^c_\alpha = p^e_\alpha + p^m_\alpha + q_\alpha - \mathrm{div}(\mathbf{q}^s_\alpha) \tag{1.1}$$

Kinetic energy density ($J.m^{-3}$) is expressed as a function of local velocity $\mathbf{v}_\alpha$ and mass density ρ_α :

$$e^c_\alpha = \frac{1}{2}\rho_\alpha \mathbf{v}_\alpha . \mathbf{v}_\alpha \tag{1.2}$$

Its time derivative reads[2]:

$$\dot{e}^c_\alpha = \rho_\alpha \mathbf{v}_\alpha . \mathbf{\Gamma}_\alpha \tag{1.3}$$

where $\mathbf{\Gamma}_\alpha$ is the local acceleration.

1. The modelling applies to single or multiphased materials where one phase at minimum is ferro(ferri)magnetic but remains at constant volume fraction. Extension to phase change is possible and applies for magnetic shape memory alloys for example.
2. The application of mass conservation relationship allows the mass density variation not to be considered in the derivation.

The mechanical power density is a function of body forces $\mathbf{f}_\alpha$, Cauchy stress tensor $\boldsymbol{\sigma}_\alpha$ and deformation rate tensor $\dot{\boldsymbol{\epsilon}}_\alpha$ following:

$$p_\alpha^m = \mathbf{f}_\alpha.\mathbf{v}_\alpha - \mathbf{div}(\boldsymbol{\sigma}_\alpha).\mathbf{v}_\alpha + \boldsymbol{\sigma}_\alpha : \dot{\boldsymbol{\epsilon}}_\alpha \tag{1.4}$$

The electromagnetic power density expression comes from the flux of Poynting vector whose local expression is given by[3]:

$$p_\alpha^e = -\mathrm{div}(\mathbf{E}'_\alpha \wedge \mathbf{H}'_\alpha) = \frac{\partial \mathbf{B}_\alpha}{\partial t}.\mathbf{H}'_\alpha + \mathbf{J}'_\alpha.\mathbf{E}'_\alpha + \frac{\partial \mathbf{D}_\alpha}{\partial t}.\mathbf{E}'_\alpha \tag{1.5}$$

where $\mathbf{J}'_\alpha$, $\mathbf{E}'_\alpha$ and $\mathbf{H}'_\alpha$ are the convective electrical current density, electrical field and magnetic field, taking account of the velocity of medium [3]. Indeed, convective electrical current density, electrical field and magnetic field are related to electrical charge density ρ_α^e, electrical current density $\mathbf{J}_\alpha$, electrical field $\mathbf{E}_\alpha$, magnetic field $\mathbf{H}_\alpha$, magnetic induction $\mathbf{B}_\alpha$, electrical induction $\mathbf{D}_\alpha$ and velocity by:

$$\begin{aligned} \mathbf{J}'_\alpha &= \mathbf{J}_\alpha + \rho_\alpha^e \mathbf{v}_\alpha \\ \mathbf{E}'_\alpha &= \mathbf{E}_\alpha + \mathbf{B}_\alpha \wedge \mathbf{v}_\alpha \\ \mathbf{H}'_\alpha &= \mathbf{H}_\alpha - \mathbf{D}_\alpha \wedge \mathbf{v}_\alpha \end{aligned} \tag{1.6}$$

After a few calculations, the following expression of electromagnetic power density is obtained.

$$p_\alpha^e = \frac{\partial \mathbf{B}_\alpha}{\partial t}.\mathbf{H}_\alpha + \frac{\partial \mathbf{D}_\alpha}{\partial t}.\mathbf{E}_\alpha + \mathbf{E}_\alpha.\mathbf{J}_\alpha + (\mathbf{J}_\alpha \wedge \mathbf{B}_\alpha + \rho_\alpha^e \mathbf{E}_\alpha + \frac{\partial}{\partial t}(\mathbf{D}_\alpha \wedge \mathbf{B}_\alpha)).\mathbf{v}_\alpha \tag{1.7}$$

Classical magnetic power, electrical power and Joule effect are the three first terms. It is remarkable that the last term $\mathbf{f}_\alpha^{em}.\mathbf{v}_\alpha$ ressembles a mechanical power, where the electromagnetic body force $\mathbf{f}^{em}$ is given by:

$$\mathbf{f}_\alpha^{em} = \mathbf{J}_\alpha \wedge \mathbf{B}_\alpha + \rho_\alpha^e \mathbf{E}_\alpha + \frac{\partial}{\partial t}(\mathbf{D}_\alpha \wedge \mathbf{B}_\alpha) \tag{1.8}$$

The Lorentz force can be recognized is this expression. This body force is usually related to the so-called Maxwell stress tensor $\boldsymbol{\sigma}_\alpha^M$ by a divergence operation:

$$\mathbf{f}_\alpha^{em} = \mathbf{div}(\boldsymbol{\sigma}_\alpha^M) \tag{1.9}$$

Finally, all quantities are introduced in the energy conservation equation leading to:

3. $\frac{\partial .}{\partial t}$ indicates a partial derivative over time. It differs from dotted quantities since dotted quantities include the convective part of time derivation.

$$\begin{aligned} \dot{u}_\alpha + \left[\rho_\alpha \mathbf{\Gamma}_\alpha - \mathbf{f}_\alpha^{em} - \mathbf{f}_\alpha - \mathbf{div}(\boldsymbol{\sigma}_\alpha)\right].\mathbf{v}_\alpha = \\ \boldsymbol{\sigma}_\alpha : \dot{\boldsymbol{\epsilon}}_\alpha + \frac{\partial \mathbf{B}_\alpha}{\partial t}.\mathbf{H}_\alpha + \frac{\partial \mathbf{D}_\alpha}{\partial t}.\mathbf{E}_\alpha + \mathbf{E}_\alpha.\mathbf{J}_\alpha + q_\alpha^s - \mathrm{div}(\mathbf{q}_\alpha^s) \end{aligned} \tag{1.10}$$

We recognize in this expression the linear momentum balance equation:

$$\rho_\alpha \mathbf{\Gamma}_\alpha - \mathbf{f}_\alpha^{em} - \mathbf{f}_\alpha - \mathbf{div}\boldsymbol{\sigma}_\alpha = \mathbf{0} \tag{1.11}$$

This equation applies at each point of a medium. Complemented by boundary conditions (surface -applied- forces or displacements), the mechanical problem can be solved leading to a stress field $\boldsymbol{\sigma}_\alpha$. If only electromagnetic body forces apply, stress (if remaining below the yield stress) lead to an elastic deformation field $\boldsymbol{\epsilon}_\alpha^e$ in the medium verifying:

$$\boldsymbol{\epsilon}_\alpha^e = C_\alpha^{-1} : \boldsymbol{\sigma}_\alpha$$

with C_α the fourth-rank local stiffness tensor of the medium. This deformation is the so-called form effect, always superimposed to the magnetostriction strain in magnetic materials.

1.2.3 Gibbs free energy at the domain scale and second law of thermodynamics - reversible framework[4]

The other consequence of the application of linear momentum balance equation is the simplification of the first law of thermodynamics. If we do not consider the dielectric power, convection phenomena (so that partial time derivation equals total time derivation: $\frac{\partial a}{\partial t} = \dot{a}$), the contribution of the magnetic field to the total power (it is present even in the absence of magnetisation), and use the decomposition $\mathbf{B}_\alpha = \mu_0(\mathbf{H}_\alpha + \mathbf{M}_\alpha)$ (with μ_0 the vacuum magnetic permeability and $\mathbf{M}_\alpha$ the local magnetisation), the first law of thermodynamics becomes:

$$\dot{u}_\alpha = \boldsymbol{\sigma}_\alpha : \dot{\boldsymbol{\epsilon}}_\alpha + \mu_0 \dot{\mathbf{M}}_\alpha.\mathbf{H}_\alpha + \mathbf{E}_\alpha.\mathbf{J}_\alpha + q_\alpha - \mathrm{div}(\mathbf{q}_\alpha^s) \tag{1.12}$$

The second law of thermodynamics states that:

$$T_\alpha \dot{s}_\alpha \geq q_\alpha - \mathrm{div}(\mathbf{q}_\alpha^s) + \frac{1}{T_\alpha}\mathbf{q}_\alpha^s.\mathbf{grad}\, T_\alpha \tag{1.13}$$

with T_α the local temperature and s_α the entropy density. Introducing the Helmholtz free energy density,

$$\psi_\alpha = u_\alpha - T_\alpha s_\alpha \tag{1.14}$$

the so-called Clausius-Duhem inequality is obtained and decomposed in intrinsic (1.15) and extrinsic (1.16) parts following [4]:

4. This subsection and the next one are largely inspired by [5]

$$\boldsymbol{\sigma}_\alpha : \dot{\boldsymbol{\epsilon}}_\alpha + \mu_0 \dot{\mathbf{M}}_\alpha . \mathbf{H}_\alpha - (s_\alpha \dot{T}_\alpha + \dot{\psi}_\alpha) \geq 0 \tag{1.15}$$

$$\mathbf{E}_\alpha . \mathbf{J}_\alpha - \frac{1}{T_\alpha} \mathbf{q}_\alpha^s . \mathbf{grad}\, T_\alpha \geq 0 \tag{1.16}$$

The Joule effect belongs to the second equation corresponding to an electrical charge transfer phenomenon. Ohm law can for example be used, ensuring that the scalar product is always positive. Joule effect acts as a heat source in the heat equation. Thermal effects are not considered in the following making consequently the extrinsic inequality (1.16) unused. Helmholtz free energy is a function of deformation, magnetisation and temperature as control variables $\psi_\alpha = \psi_\alpha(\boldsymbol{\epsilon}_\alpha, \mathbf{M}_\alpha, T_\alpha)$. The associated power is consequently:

$$\dot{\psi}_\alpha = \frac{\partial \psi_\alpha}{\partial \boldsymbol{\epsilon}_\alpha} : \dot{\boldsymbol{\epsilon}}_\alpha + \frac{\partial \psi_\alpha}{\partial \mathbf{M}_\alpha} . \dot{\mathbf{M}}_\alpha + \frac{\partial \psi_\alpha}{\partial T_\alpha} \dot{T}_\alpha \tag{1.17}$$

Let consider now a reversible framework. The assumption of reversible behaviour states that the intrinsic part of Clausius-Duhem inequality is null, leading to the so-called thermodynamic consistency equations (1.18).

$$\boldsymbol{\sigma}_\alpha = \frac{\partial \psi_\alpha}{\partial \boldsymbol{\epsilon}_\alpha} \quad ; \quad \mathbf{H}_\alpha = \frac{\partial \psi_\alpha}{\mu_0 \partial \mathbf{M}_\alpha} \quad ; \quad s_\alpha = -\frac{\partial \psi_\alpha}{\partial T_\alpha} \tag{1.18}$$

Therefore, the Helmholtz free energy variation (for a time step dt) is controlled by magnetisation and total deformation variations at constant temperature:

$$d\psi_\alpha = \boldsymbol{\sigma}_\alpha : d\boldsymbol{\epsilon}_\alpha + \mu_0 \mathbf{H}_\alpha . d\mathbf{M}_\alpha \tag{1.19}$$

The magnetic free enthalpy (Legendre transformation of magnetic quantity) $\kappa_\alpha = \psi_\alpha - \mu_0 \mathbf{H}_\alpha . \mathbf{M}_\alpha$ allows the energy variation to be defined as a function of magnetic field variation instead of magnetisation variation. The Gibbs free energy (or free enthalpy) (Legendre transformation of mechanical quantity) $\mathfrak{g}_\alpha = \kappa_\alpha - \boldsymbol{\sigma}_\alpha : \boldsymbol{\epsilon}_\alpha$ allows finally the energy variation to be defined as function of stress variation instead of deformation variation. Variation of Gibbs free energy is given by:

$$d\mathfrak{g}_\alpha = -\boldsymbol{\epsilon}_\alpha : d\boldsymbol{\sigma}_\alpha - \mu_0 \mathbf{M}_\alpha . d\mathbf{H}_\alpha \tag{1.20}$$

Strain and magnetisation finally derive from the Gibbs free energy function following:

$$\boldsymbol{\epsilon}_\alpha = -\frac{\partial \mathfrak{g}_\alpha}{\partial \boldsymbol{\sigma}_\alpha} \quad ; \quad \mathbf{M}_\alpha = -\frac{\partial \mathfrak{g}_\alpha}{\mu_0 \partial \mathbf{H}_\alpha} \tag{1.21}$$

Small perturbation hypothesis allows the total deformation to be considered as a sum of elastic $\boldsymbol{\epsilon}_\alpha^e$ and inelastic part. The inelastic part being supposed to be

related to the magnetic loading via a constitutive law, it is called magnetostriction strain and denoted $\boldsymbol{\epsilon}_\alpha^\mu$. The decomposition leads to:

$$\boldsymbol{\epsilon}_\alpha = \boldsymbol{\epsilon}_\alpha^e + \boldsymbol{\epsilon}_\alpha^\mu = C_\alpha^{-1} : \boldsymbol{\sigma}_\alpha + \boldsymbol{\epsilon}_\alpha^\mu \tag{1.22}$$

$\boldsymbol{\epsilon}_\alpha^\mu$ may depend at this step on magnetic field and stress at the local scale so that the derivation of the mechanical part of the Gibbs free energy involves an integration of magnetostriction strain over the stress path:

$$\mathfrak{g}_\alpha^{mech} = -\frac{1}{2}\boldsymbol{\sigma}_\alpha : C_\alpha^{-1} : \boldsymbol{\sigma}_\alpha - \int_{\mathbf{0}}^{\boldsymbol{\sigma}_\alpha} \boldsymbol{\epsilon}_\alpha^\mu : d\boldsymbol{\sigma}_\alpha \tag{1.23}$$

For the derivation of the magnetic part of the Gibbs free energy, Helmholtz magnetic free energy ψ_α^{magn} is usually defined as a Taylor expansion of magnetisation (sixth order expansion), taking into account the fact that the magnetic behaviour is an odd function of magnetisation. Second-rank $\mathbf{K}_\alpha$, fourth-rank $\mathcal{K}_\alpha$ and sixth-rank $\mathbb{K}_\alpha$ tensors are used to define the magneto-crystalline part of Helmholtz free energy. Their expressions are strongly correlated to material symmetries. The coupling between neighbouring atoms leads to a constant magnetisation direction over a wide volume (i.e. magnetic domains). Any angular deviation leads to an energy increase, known as the exchange energy, whose expression involves the magnetisation gradient $\mathbf{grad}\,\mathbf{M}_\alpha$ and an exchange constant A in the framework of continuum mechanics. The expression of Gibbs magnetic free energy (after Legendre transformation) is finally given by:

$$\begin{aligned}\mathfrak{g}_\alpha^{mag} = \tfrac{A}{M_\alpha^2}\mathbf{grad}\,\mathbf{M}_\alpha : \mathbf{grad}\,\mathbf{M}_\alpha + \mathbf{M}_\alpha.\mathbf{K}_\alpha.\mathbf{M}_\alpha + \mathbf{M}_\alpha \otimes \mathbf{M}_\alpha : \mathcal{K}_\alpha : \mathbf{M}_\alpha \otimes \mathbf{M}_\alpha \\ + \mathbf{M}_\alpha.(\mathbf{M}_\alpha \otimes \mathbf{M}_\alpha : \mathbb{K}_\alpha : \mathbf{M}_\alpha \otimes \mathbf{M}_\alpha).\mathbf{M}_\alpha - \mu_0 \mathbf{H}_\alpha.\mathbf{M}_\alpha\end{aligned} \tag{1.24}$$

The sum of $\mathfrak{g}_\alpha^{mech}$ and $\mathfrak{g}_\alpha^{mag}$ gives the total Gibbs free energy of the medium. It must be minimum with respect to stress and magnetic field at the equilibrium. It must be noticed that the magneto-mechanical part of the mechanical Gibbs free energy could be defined in the frame of magnetic Gibbs free energy expression using a Taylor expansion as well. Indeed this term denotes the coupling between magnetics and mechanics. Its expression is key for an appropriate modelling.

1.2.4 Simplification of Gibbs free energy at the domain scale - cubic symmetry

Following the proposed scaling (section 1.2.1), α denotes a domain family (or more simply a *domain*). The number of domain families is defined by the number of easy magnetic axes in the crystal (6 directions for $< 100 >$ easy axes materials, and 8 directions for $< 111 >$ easy axes materials). First, it is interesting to observe that the magnetisation at the domain scale oriented along an

axis $\boldsymbol{\alpha}$ has a constant norm equal to the saturation magnetisation M_s. The magnetisation vector can be defined using the direction cosines α_i in the local frame (usually crystal frame $\mathbf{e}_i$) as:

$$\mathbf{M}_\alpha = M_s \boldsymbol{\alpha} = M_s \, {}^t[\alpha_1 \ \alpha_2 \ \alpha_3] = M_s \alpha_i \mathbf{e}_i \tag{1.25}$$

In a magnetic domain, spatial variations of magnetisation are inexistent, the magnetisation gradient is consequently zero. The Gibbs free energy (average energy density over a domain) can consequently be simplified but will not allow the domain walls to be described [5].
The dyadic product of $\mathbf{M}_\alpha$ allows the second-rank orientation tensor $\mathbf{R}_\alpha$ to be defined :

$$\mathbf{M}_\alpha \otimes \mathbf{M}_\alpha = M_s^2 \, \boldsymbol{\alpha} \otimes \boldsymbol{\alpha} = M_s^2 \begin{pmatrix} \alpha_1^2 & \alpha_1\alpha_2 & \alpha_1\alpha_3 \\ \alpha_1\alpha_2 & \alpha_2^2 & \alpha_2\alpha_3 \\ \alpha_1\alpha_3 & \alpha_2\alpha_3 & \alpha_3^2 \end{pmatrix} = M_s^2 \mathbf{R}_\alpha \tag{1.26}$$

Using the cubic symmetry and the identity $\sum_i \alpha_i \alpha_i = 1$, the magnetic part of Gibbs free energy simplifies into:

$$\mathfrak{g}_\alpha^{mag} = K_0 + K_1(\alpha_1^2\alpha_2^2 + \alpha_1^2\alpha_3^2 + \alpha_2^2\alpha_3^2) + K_2(\alpha_1^2\alpha_2^2\alpha_3^2) - \mu_0 \mathbf{H}_\alpha . \mathbf{M}_\alpha \tag{1.27}$$

where K_0, K_1 and K_2 are the so-called magnetocrystalline constants (defining the magnetocrystalline -non convex- energy density) and the last term is usually called Zeemann energy density (if $\mathbf{H}_\alpha$ is considered homogeneous).

The mechanical part of the Gibbs free energy may be simplified at the domain scale by using the so-called magnetostriction tensor of a domain α defined by:

$$\boldsymbol{\epsilon}_\alpha^\mu = \frac{3}{2} \begin{pmatrix} \lambda_{100}(\alpha_1^2 - \frac{1}{3}) & \lambda_{111}\alpha_1\alpha_2 & \lambda_{111}\alpha_1\alpha_3 \\ \lambda_{111}\alpha_1\alpha_2 & \lambda_{100}(\alpha_2^2 - \frac{1}{3}) & \lambda_{111}\alpha_2\alpha_3 \\ \lambda_{111}\alpha_1\alpha_3 & \lambda_{111}\alpha_2\alpha_3 & \lambda_{100}(\alpha_3^2 - \frac{1}{3}) \end{pmatrix} \tag{1.28}$$

where λ_{100} and λ_{111} are the magnetostriction constants that correspond to the deformation of a perfect single crystal along $< 100 >$ and $< 111 >$ axes respectively at the magnetic saturation. This tensor is considered independent to stress and leads to the following reformulation of the mechanical part of the Gibbs free energy by allowing the integral term to be simplified[6]:

5. This is addressed by micromagnetic formulations as briefly recalled in chapter "Multi-scale modelling of magnetic materials".
6. This simplification is especially encountered in the construction of macroscopic models but not always justified.

$$\mathfrak{g}_\alpha^{mech} = -\frac{1}{2}\boldsymbol{\sigma}_\alpha : C_\alpha^{-1} : \boldsymbol{\sigma}_\alpha - \boldsymbol{\sigma}_\alpha : \boldsymbol{\epsilon}_\alpha^\mu \tag{1.29}$$

1.2.5 Second law of thermodynamics - irreversible framework

An appropriate expression of magnetic Gibbs free energy allows theoretically an appropriate reversible (*anhysteretic*) behaviour to be obtained. The magnetic behaviour however is never reversible even in quasi-static condition. The description of the non-reversible (irreversible) part of the behaviour follows different strategies: decomposition of magnetisation in reversible and irreversible parts (Jiles-Atherton model), decomposition of magnetic field in reversible and irreversible parts (Schneider, Hauser), or without reversible term (Preisach) [6]. All propositions must satisfy however the second law of thermodynamics. Expressions are given at the local (domain) scale below. They of course apply at the macroscale, joining the various macroscopic descriptions of dissipation proposed in literature.

The instrinsic part of Clausius-Duhem inequality is recalled (see eq. 1.15):

$$\boldsymbol{\sigma}_\alpha : \dot{\boldsymbol{\epsilon}}_\alpha + \mu_0 \dot{\mathbf{M}}_\alpha . \mathbf{H}_\alpha - (s_\alpha \dot{T}_\alpha + \dot{\psi}_\alpha) \geq 0 \tag{1.30}$$

Restricted to the magnetic behaviour, the second law of thermodynamics simplifies into:

$$\mu_0 \dot{\mathbf{M}}_\alpha . \mathbf{H}_\alpha - \dot{\psi}_\alpha \geq 0 \tag{1.31}$$

The simplest situation is the situation where the magnetic power is totally dissipated (no stored energy). The variation of Helmholtz energy is consequently null. Magnetic quantities must verify:

$$\mu_0 \dot{\mathbf{M}}_\alpha . \mathbf{H}_\alpha \geq 0 \tag{1.32}$$

This situation is however unphysical. A part of magnetic energy is always stored. The Helmholtz free energy description is suitable for a partition in irreversible and reversible magnetisation ($\mathbf{M}_\alpha = \mathbf{M}_\alpha^{rev} + \mathbf{M}_\alpha^{irr}$ and $\psi_\alpha(\mathbf{M}_\alpha) = \psi_\alpha(\mathbf{M}_\alpha^{rev})$) so that variables should verify:

$$\begin{aligned} \mathbf{H}_\alpha &= \frac{\partial \psi_\alpha}{\mu_0 \partial \mathbf{M}_\alpha^{rev}} \\ \mu_0 \dot{\mathbf{M}}_\alpha^{irr} . \mathbf{H}_\alpha &\geq 0 \end{aligned} \tag{1.33}$$

The Gibbs free energy is however more suitable for a magnetic field controlled problem. Quantities must then verify:

$$-\mu_0 \mathbf{M}_\alpha . \dot{\mathbf{H}}_\alpha - \dot{\mathfrak{g}}_\alpha \geq 0 \tag{1.34}$$

Indeed the Gibbs free energy description is suitable for a partition in irreversible and reversible magnetic field ($\mathbf{H}_\alpha = \mathbf{H}_\alpha^{rev} + \mathbf{H}_\alpha^{irr}$ and $\mathfrak{g}_\alpha(\mathbf{H}_\alpha) = \mathfrak{g}_\alpha(\mathbf{H}_\alpha^{rev})$) so that the variables should verify:

$$\begin{aligned} \mathbf{M}_\alpha &= -\frac{\partial \mathfrak{g}_\alpha}{\mu_0 \partial \mathbf{H}_\alpha^{rev}} \\ -\mu_0\, \mathbf{M}_\alpha . \dot{\mathbf{H}}_\alpha^{irr} &\geq 0 \end{aligned} \tag{1.35}$$

The instrinsic part of Clausius-Duhem inequality includes a mechanical term (eq. 1.30), for which a dissipation can be considered as well. It is well known that plasticity is a source of mechanical energy dissipation, even if a part of energy associated with plastic deformation is stored (dislocations, residual stresses). In a magneto-elastic problem, magnetostriction represents the inelastic part of the deformation. As for plasticity, the associated energy can be either stored or released.

Restricting to the mechanical behaviour, and removing, for the sake of simplicity, the elastic part of the deformation (which is always stored), the second law of thermodynamics simplifies into[7]:

$$\boldsymbol{\sigma}_\alpha : \dot{\boldsymbol{\epsilon}}_\alpha^\mu + \dot{\psi}_\alpha^\mu \geq 0 \tag{1.36}$$

The Helmholtz free energy description is suitable for a partition into irreversible and reversible magnetostriction ($\boldsymbol{\epsilon}_\alpha^\mu = \boldsymbol{\epsilon}_\alpha^{\mu-rev} + \boldsymbol{\epsilon}_\alpha^{\mu-irr}$ and $\psi_\alpha^\mu(\boldsymbol{\epsilon}_\alpha^\mu) = \psi_\alpha^\mu(\boldsymbol{\epsilon}_\alpha^{\mu-rev})$) so that the variables should verify:

$$\begin{aligned} \boldsymbol{\sigma}_\alpha &= \frac{\partial \psi_\alpha^\mu}{\partial \boldsymbol{\epsilon}_\alpha^{\mu-rev}} \\ \boldsymbol{\sigma}_\alpha &: \dot{\boldsymbol{\epsilon}}_\alpha^{\mu-irr} \geq 0 \end{aligned} \tag{1.37}$$

As for the magnetic behaviour, Gibbs free energy is more suitable for a stress controlled problem. Quantities must then verify:

$$-\dot{\boldsymbol{\sigma}}_\alpha : \boldsymbol{\epsilon}_\alpha^\mu - \dot{\mathfrak{g}}_\alpha^\mu \geq 0 \tag{1.38}$$

This formulation is now suitable for a partition into irreversible and reversible stress ($\boldsymbol{\sigma}_\alpha = \boldsymbol{\sigma}_\alpha^{rev} + \boldsymbol{\sigma}_\alpha^{irr}$ and $\mathfrak{g}_\alpha^\mu(\boldsymbol{\sigma}_\alpha) = \mathfrak{g}_\alpha^\mu(\boldsymbol{\sigma}_\alpha^{rev})$) so that the variables should verify[8]:

$$\begin{aligned} \boldsymbol{\epsilon}_\alpha^\mu &= -\frac{\partial \mathfrak{g}_\alpha^\mu}{\partial \boldsymbol{\sigma}_\alpha^{rev}} \\ -\dot{\boldsymbol{\sigma}}_\alpha^{irr} &: \boldsymbol{\epsilon}_\alpha^\mu \geq 0 \end{aligned} \tag{1.39}$$

During quasistatic magnetisation, the pinning mechanism of domain walls and wall jumps are the main source of energy dissipation. It depends only on the

7. The notation $\dot{\psi}_\alpha^\mu$ indicates that the energy is restricted to the magnetomechanical term.
8. The notation $\dot{\mathfrak{g}}_\alpha^\mu$ indicates that we restrict the Gibbs energy to the magnetomechanical term.

path made by the walls and does not depend on whether the wall displacement is generated by the application of a magnetic field or a mechanical stress. This simply justifies the relevance of including an irreversible term in the magneto-elastic energy. Stress-induced magnetostriction cycle (stress vs magnetostriction) can hardly be obtained experimentally. The more relevant indicator of the effect of a variable stress is the *piezomagnetic* cycle (magnetisation $\mathbf{M}$ vs. stress $\boldsymbol{\sigma}$ cycle). Once homogenised at the macroscale, the proposed formulation is able to give a framework for an appropriate modelling of piezomagnetic cycles. It must be underlined on the other hand that following the previous remarks and discussion, a piezomagnetic cycle that mixes two variables (magnetisation $\mathbf{M}$ and stress $\boldsymbol{\sigma}$) that are not thermodynamically associated, is not representative of an energy dissipation, unlike a magnetostriction vs. stress cycle.

1.3 MULTISCALE MODELLING

1.3.1 Constitutive behaviour, localisation and homogenisation

The objective of the multiscale approach is to calculate, through scale transition procedures, the macroscopic magnetisation $\mathbf{M}$ and magnetostriction $\boldsymbol{\epsilon}^{\mu}$ as functions of macroscopic magnetic field $\mathbf{H}$ and stress $\boldsymbol{\sigma}$. Localization (from the macroscale to the domain scale) and homogenisation (from domain scale to macroscale) steps are required, and the constitutive behaviour is defined at the local (domain) scale [7, 8].

$\mathbf{H}_{\alpha}$ is the magnetic field at the domain scale. $\boldsymbol{\sigma}_{\alpha}$ is the stress tensor at the domain scale. Assumptions of homogeneous field and stress at the grain scale (1.40) lead to a stronger simplification of the Gibbs free energy (1.41) (purely mechanical terms are removed).

$$\mathbf{H}_{\alpha} = \mathbf{H}_{g} \quad ; \quad \boldsymbol{\sigma}_{\alpha} = \boldsymbol{\sigma}_{g} \tag{1.40}$$

$$\begin{aligned} \mathfrak{g}_{\alpha} = -\tfrac{1}{2}\boldsymbol{\sigma}_{g} : C_{g}^{-1} : \boldsymbol{\sigma}_{g} \; - \; \boldsymbol{\sigma}_{g} : \boldsymbol{\epsilon}_{\alpha}^{\mu} + K_1(\alpha_1^2\alpha_2^2 + \alpha_1^2\alpha_3^2 + \alpha_2^2\alpha_3^2) \\ + K_2(\alpha_1^2\alpha_2^2\alpha_3^2) - \mu_0 \mathbf{H}_{g}.\mathbf{M}_{\alpha} \end{aligned} \tag{1.41}$$

Once the Gibbs free energy $\mathfrak{g}_{\alpha}$ is known for a given domain family α of direction $\boldsymbol{\alpha} = [cos\theta_{\alpha} sin\phi_{\alpha}; sin\theta_{\alpha} sin\phi_{\alpha}; cos\phi_{\alpha}]$, its volume fraction f_{α} (1.42) is calculated according to an explicit Boltzmann-type relation. This stochastic approach is relevant since the volume considered is sufficient, assuming that a magnetic domain is much smaller than a representative volume element (considered as a small body immersed into a large closed thermodynamic system). Numerical results should consequently be compared to experimental results obtained *at equilibrium*. A_s (1.43) is an adjusting parameter related to the initial magnetic susceptibility χ_0 of the material in absence of external loading. This

calculation is complemented by an energy minimization (1.44) for the determination of the magnetisation direction $\boldsymbol{\alpha}$. This formulation is well suited for a single variant and single phase ferromagnetic material (ferromagnetic ferrite or austenite, ferrimagnetic materials, rare-earth materials such as Terfenol or Galfenol)[9].

$$f_\alpha = \frac{\exp(-A_s\, \mathfrak{g}_\alpha)}{\sum_\beta \exp(-A_s\, \mathfrak{g}_\beta)} \tag{1.42}$$

with

$$A_s = \frac{3\chi_0}{\mu_0 M_s^2} \tag{1.43}$$

$$\{\theta_\alpha, \phi_\alpha\} = \arg\min(\mathfrak{g}_\alpha) \tag{1.44}$$

Assuming that the elastic behaviour and the magnetic susceptibility are homogeneous within a grain, the magnetostriction strain and the magnetisation of a single crystal are written as the average magnetostriction and magnetisation over the domains (1.45) and (1.46).

$$\boldsymbol{\epsilon}_g^\mu = <\boldsymbol{\epsilon}_\alpha^\mu> = \sum_\alpha f_\alpha\, \boldsymbol{\epsilon}_\alpha^\mu \tag{1.45}$$

$$\mathbf{M}_g = <\mathbf{M}_\alpha> = \sum_\alpha f_\alpha\, \mathbf{M}_\alpha \tag{1.46}$$

This calculation has to be made for each grain of a polycrystalline aggregate. Since grains are not isotropic and are disoriented from each other, localisation rules are required to define the stress and magnetic fields at the grain scale as a function of macroscopic loadings. An Eshelby approach can be applied for the determination of both fields. The orientation of a grain inside the polycrystalline medium can be defined by three Euler angles, which are different from one grain to another. The local magnetisation and deformation are different from one grain to another. Local magnetic and mechanical loadings ($\mathbf{H}_g$ and $\boldsymbol{\sigma}_g$) are then different from the macroscopic loadings ($\mathbf{H}$ and $\boldsymbol{\sigma}$). Typically the calculation of the local loadings is carried out on each grain through a self-consistent polycrystalline scheme [8], where loadings at the grain scale are derived from the macroscopic loadings, using equations (1.47) and (1.58). The gap between local and global quantities defines the demagnetising field and the residual stress.

9. More complex formulation can be proposed to take a possible phase transformation (ferromagnetic to ferromagnetic, or ferromagnetic to paramagnetic) or the existence of several variants into account. The total number of internal variables strongly depends on the number of grains, phases, variants and number of domain families inside each variant.

$$\mathbf{H}_g = \mathbf{H} + \frac{1}{3 + 2\chi_m}(\mathbf{M} - \mathbf{M}_g) \tag{1.47}$$

χ_m is the secant magnetic susceptibility ($\chi_m = \|\mathbf{M}\|/\|\mathbf{H}\|$),

$$\boldsymbol{\sigma}_g = \mathcal{B}_g : \boldsymbol{\sigma} + \mathcal{C}^{acc} : (\boldsymbol{\epsilon}^{\mu} - \boldsymbol{\epsilon}^{\mu}_g) \tag{1.48}$$

where the accomodation stiffness tensor $\mathcal{C}^{acc}$ and the stress concentration tensor $\mathcal{B}_g$ can be determined from Hill's constraint tensor, the stiffness tensor of the effective medium and the stiffness tensor of the grain.

The self-consistent approach is implicit as the definition of stress and magnetic field at the grain scale ($\mathbf{H}_g$ and $\boldsymbol{\sigma}_g$) involve the corresponding local ($\mathbf{M}_g$, $\boldsymbol{\epsilon}^{\mu}_g$) and macroscopic quantities :

$$\mathbf{M} = < \mathbf{M}_g > \tag{1.49}$$

$$\boldsymbol{\epsilon}^{\mu} = < {}^t\mathcal{B}_g : \boldsymbol{\epsilon}^{\mu}_g > \tag{1.50}$$

This can be resolved through an iterative procedure. Once convergence is reached local and global quantities are known.

Different materials can be modelled by this approach provided that they consist of crystals of which at least one family is ferromagnetic or ferrimagnetic. The mixture of properties is not a problem since the properties of each of the constituents (saturation magnetisation, magnetocrystalline anisotropy, magnetostrictive constants, stiffness) and orientation of crystals (Euler angles) are known. It is also possible to consider a situation where the proportion of magnetic phase evolves relatively to a nonmagnetic phase (phase transformation situation). Moreover, this approach allows dealing with the effects of plasticity on magnetic behaviour by considering plasticity through the residual stresses it introduces in the deformed material [9].

1.3.2 Taking into account an initial unbalanced distribution of magnetic domains

The thermomechanical history of a material, from its elaboration to its implementation in a system, is often complex. It induces phenomenons that the multiscale model in its standard version can take into account for most of them: crystallographic texture, mixture of phases, residual stresses field, plasticity. However, the model considers that, in the absence of loading, the domain structure is always balanced. This is clearly not the case in materials such as Grain-Oriented 3%Si-Fe alloys and most laminated materials, inheriting chemical fluctuations, which, coupled with the local magnetic field, lead to an unbalanced distribution of the domain structure. The introduction of such physics in the modelling is currently out of reach. Yet, a partial consideration of surface or chemical

anisotropy phenomena is possible through the introduction of some specific potentials added to Gibbs free energy [10].

In the case of large grain size vs. thickness ratio, the emerging component of the magnetisation is very unfavorable because of the presence of two free surfaces (only a small misorientation is enough to disturb the domain configuration). A specific surface energy term (eq 1.51) can be added to the Gibbs free energy of a domain family (eq. 1.41).

$$\mathfrak{g}_\alpha^S = N_s(\boldsymbol{\alpha}.\mathbf{z}_0)^2 \tag{1.51}$$

$\mathbf{z}_0$ is the direction normal to the sheet plane and N_s a demagnetising field factor that defines the maximum level of the surface energy. This energy term acts as a macroscopic uniaxial anisotropy energy. It is possible to generalize this form to triaxial anisotropy (eq. 1.52).

$$\mathfrak{g}_\alpha^S = C\,{}^t\boldsymbol{\alpha}.\mathbf{N}.\boldsymbol{\alpha} \tag{1.52}$$

where $\mathbf{N}$ is an a-dimensional anisotropy matrix, and C a constant ($\mathrm{J.m^{-3}}$). This anisotropy matrix is diagonal in the principal framework associated with the medium. Each term of matrix $\mathbf{N}$ can be analytically calculated if some hypotheses are made about the behaviour (supposed most of the time linear), about the surrounding magnetisation (supposed most of the time null) and about the shape (supposed most of the time ellipsoidal). It is possible to find some guidelines for the evaluation of $\mathbf{N}$ depending on sample geometry and grain size vs. sample size ratio.

On the other hand, it may be possible to link the expression of $\mathfrak{g}_\alpha^S$ to the usual magnetostatic energy. Surface effect can be seen as the effect of a macroscopic demagnetising field acting on each domain. The existence of a demagnetising field at this scale is in discordance with the hypothesis of homogeneous magnetic field ($\mathbf{H}_\alpha = \mathbf{H}_g$). It is nevertheless possible to define a new localisation law from the grain to the domain scale following equation (1.47):

$$\mathbf{H}_\alpha = \mathbf{H}_g + C_0\,\mathbf{N}.(\mathbf{M}_g - \mathbf{M}_\alpha) \approx \mathbf{H}_g - C_0\mathbf{N}.\mathbf{M}_\alpha \tag{1.53}$$

where C_0 is an a-dimensional fitting constant. In this equation, the magnetisation at grain scale is considered negligible compared to the magnetisation at domain scale. This is a very rough simplification. But it allows an expression to be obtained where the demagnetising field at the domain scale is constant:

$$\mathbf{H}_\alpha^d = -C_0\,\mathbf{N}.\mathbf{M}_\alpha \tag{1.54}$$

The approach developed above can be extended to any type of situation where thermo-magneto-mechanical history has led to an unbalanced configuration. It is thus possible to propose a general form (potential) that could generate this situation. This potential must however respect the centrosymmetry

associated with magnetism, based, for example, on a even function of the local magnetisation vector. A quadratic function of local magnetisation vector requires the introduction of a second-rank $\mathbf{Q}$ a-dimensional configuration matrix. The associated so-called configuration potential can read:

$$\mathfrak{g}_{\alpha}^{C} = -K_c \, {}^{t}\boldsymbol{\alpha}.\mathbf{Q}.\boldsymbol{\alpha} \tag{1.55}$$

1.3.3 Multiscale modelling of hysteresis magnetic, magnetostrictive and piezomagnetic behaviour

The multiscale approach is by definition anhysteretic, meaning that it is restricted to the reversible part of magneto-elastic behaviour. Hysteresis effects can be introduced in the multiscale model in terms of irreversible magnetic field (see chapter "Multi-scale modelling of magnetic materials"). The dissipation is introduced (initially in the single crystal model) by adding an irreversible contribution H_{irr} to the anhysteretic magnetic field H (considered as the *reversible* magnetic field H_{rev}), in accordance with the thermodynamic consistency detailed in section 1.2.5. The definition of H_{irr} is based on the works by Hauser [11], extended to magneto-mechanical loadings.
The Hauser model predicts the magnetic state of the ferromagnetic material by minimizing the overall energy state of the system. This approach is based on a physical and probabilistic description of the volume distribution of the magnetic domain families. The dissipative behaviour results from the probability of encountering a defect during the displacement of domain walls separating the magnetic domains. The expression of the irreversible energy is a decreasing exponential function which depends on the variations of the anhysteretic volume fraction. It reflects the fact that a wall has a lower probability of being pinned to a defect when it is away from it. This development is often simplified by studying a load applied along an easy magnetisation axis of the material and considering quantities as isotropic and at the macroscopic scale. Following these simplifications, equation (1.56) gives the expression of H_{irr}.

$$H_{irr} = \delta(H_c + a|H_{rev}|)\left[1 - \kappa \, \exp\left(-\frac{k_a}{\kappa}|M - M_{prev}|\right)\right] \tag{1.56}$$

where

$$\begin{aligned} \delta &= \text{sign}(M - M_{prev}) \\ \kappa &= 2 - \kappa_0 \, \exp\left(-\frac{k_a}{\kappa_0}|M - M_{prev}|\right) \end{aligned} \tag{1.57}$$

Here all fields are assumed to be parallel and a 1D representation is adopted with $H = H_{rev} + H_{irr}$. Hysteresis is restricted to magnetic field amplitude effects, rotational effects cannot be modelled. δ is equal to ± 1, depending on the loading direction. The sign of δ starts as positive and is then changed at

each inversion in loading direction. H_c denotes the coercive field of the material (magnetic field required to cancel the remanent magnetisation for a major loop). a, k_a and κ are material parameters. a controls the first magnetisation behaviour, and k_a and κ the width and inclination of the hysteresis cycle. The value of κ changes each time there is an inversion in the loading direction. The new κ value is calculated from the previous value κ_0 according to eq. (1.57). The initial κ value is a material constant. M_{prev} is the value of magnetisation M at the previous inversion of the loading direction. In the case of a purely magnetic loading, an inversion of loading direction is defined as a change of sign for the time derivative of the applied magnetic field. It can, on the other hand, be verified that the definition of irreversible magnetic field allows a positive dissipation of energy in accordance with eq. (1.35).

As explained in section 1.2.5, piezomagnetic cycle is representative of a dissipative part of magneto-mechanical energy. Using the Gibbs free energy description, and considering that phenomena explaining the magnetic dissipation apply for the piezomagnetic dissipation, the definition of an irreversible stress directly inspired form the irreversible magnetic field definition can be proposed, restricted to 1D loading at the macroscopic scale.

$$\sigma = \sigma_{rev} + \sigma_{irr} \tag{1.58}$$

with σ_{rev} the *reversible* stress leading to the equilibrium-magnetisation using the multiscale model. σ_{irr} is given by:

$$\sigma_{irr} = \delta(\sigma_C + a'|\sigma_{rev}|)\left[1 - \kappa' \exp(-\frac{k'_a}{\kappa'}|\epsilon^\mu - \epsilon^\mu_{prev}|)\right] \tag{1.59}$$

and

$$\begin{aligned} \delta &= \text{sign}(\epsilon^\mu - \epsilon^\mu_{prev}) \\ \kappa' &= 2 - \kappa'_0 \exp\left(-\tfrac{k'_a}{\kappa'_0}|\epsilon^\mu - \epsilon^\mu_{prev}|\right) \end{aligned} \tag{1.60}$$

These equations define four more material coefficients: a *coercive stress* σ_C, and parameters a', k'_a and κ'_0. a' controls the first stress-induced magnetostriction behaviour, and k'_a and κ' the width and inclination of the stress-induced magnetostriction hysteresis cycle. ϵ^μ_{prev} is the value of magnetostriction strain ϵ^μ in the direction of the applied stress at the previous inversion of the loading direction. An inversion of loading direction (leading to a change of the sign of parameter δ) is defined as a change of sign for the time derivative of the applied stress.

1.4 COMPARISON TO EXPERIMENTAL RESULTS

Some comparisons between various experiments and multiscale modelling are addressed in this section. Experiments concern magneto-mechanical effects in

different stress and magnetic field configurations. For the sake of brevity, illustrations are restricted to reversible behaviour. For all the experiments reported, the magnetic forces were previously calculated (that required a structure calculation -see chapter "Multi-scale modelling of magnetic materials") and local and global associated elastic deformations estimated. The configuration of experiments leads to a deformation field $\boldsymbol{\epsilon}^{em}$ that is at least an order of magnitude smaller than the magnetostriction strain.

1.4.1 Magnetostriction of Grain-Oriented 3%Si-Fe

Grain Oriented (GO) Silicon Iron alloys are among the most popular soft ferromagnetic materials. They exhibit the so-called GOSS texture, and are widely used in high power transformers because of their very good magnetic properties along the rolling direction. The laminations are usually stacked together and assembled. Such structures are on the other hand well known to emit vibrations and noise, a large amount of which is explained by magnetostriction strain strongly correlated to the crystallographic texture. An accurate prediction of magnetostriction anisotropy is key for optimization in order to reduce the acoustic emission. Table 1.1 gathers the constants used for the multiscale modelling [10]. Figure 1.2a shows the <100> pole figure representative of the orientation data file used for modelling (15 orientations).

«FIGURE 2 HERE»

«TABLE 1 HERE»

Figures 1.2b-c-d show the relevance of the modelling to describe the magnetic and magnetostrictive anisotropy of this material.

1.4.2 Influence of stress on magnetic and magnetostrictive behaviour of steel

The precise modelling of magnetostrictive behaviour of steels as such is not of great interest: the amplitude of the deformation is low, making steel a bad candidate for sensor or actuator applications. Steel, on the other hand, is an omnipresent material in mechanical and civil engineering. Thus, despite a low magnetostriction, the magneto-mechanical coupling is sufficient for a stress field to significantly modify the magnetic behaviour. An in situ magnetic sensor or an eddy current probe can be sensitive to these behaviour changes and thus allow a health check of the structure. We propose below to illustrate the capabilities of the multiscale model to reproduce the magnetic and magnetostrictive behaviour (longitudinal and transversal) of a low carbon steel (0.18%C) subjected to uniaxial stress [9]. Figure 1.3a shows the <100> pole figure representing the orientation data file used for modelling (299 orientations). Figures 1.4 and 1.5 allow modelling and experimental results to be compared. Multiscale approach leads to a convincing modelling of the whole magneto-mechanical behaviour.

«TABLE 2 HERE»

«FIGURE 3 HERE»

«FIGURE 4 HERE»

«FIGURE 5 HERE»

1.4.3 Piezomagnetic behaviour of Iron-Cobalt

Sensors or actuators based on piezomagnetic behaviour must use materials that show a large coupling between mechanical and magnetic properties. Specifically, the variation of the magnetisation M with respect to the applied uniaxial stress σ (i.e. $dM/d\sigma$) should be high for an appropriate sensitivity. Following the thermodynamic framework developed in previous section, the coupling leads to the thermodynamic consistency condition for macroscopic quantities (eq. 1.61). A high piezomagnetic sensitivity is reached for soft magnetic materials exhibiting a high magnetostriction amplitude. Rare earth elements (Tb, Dy) are often used as secondary elements in alloys because they exceptionally enhance the magnetomechanical properties. Their increasing price and limited availability makes the development of rare-earth-free alloys relevant.

$$\mu_0 \left.\frac{d\mathbf{M}}{d\boldsymbol{\sigma}}\right|_{\mathbf{H}} = \left.\frac{d\boldsymbol{\epsilon}^{\mu}}{d\mathbf{H}}\right|_{\boldsymbol{\sigma}} \tag{1.61}$$

Fe-Al or Fe-Co alloys demonstrated to be interesting candidates. Experimental results of piezomagnetic sensitivity of a bulk Fe-Co [12] and comparison to results coming from associated multiscale modelling are reported in figure 1.6. Constants used for multiscale modelling are given in table 1.3. Figure 1.3b shows the <100> pole figure representative of the orientation data file used for modelling (126 orientations).

«TABLE 3 HERE»

«FIGURE 6 HERE»

1.4.4 Influence of compressive stress on the magnetostriction amplitude of Terfenol-D

In applications such as low voltage actuators, large force actuators, high power low frequency transducers or structural vibration control applications, giant magnetostrictive materials can be particularly interesting. Among them, bulk Tb0.3-Dy0.7Fe1.92 (Terfenol-D) presents a large room temperature strain at relatively low magnetic field (below 40 $kA.m^{-1}$), good magneto-mechanical coupling factor, high energy density and fast response. However, this behaviour is highly nonlinear and very sensitive to mechanical loading. With structural design in

view, accurate models are needed to predict material properties under stress and to propose adapted design of Terfenol-D devices. We propose hereafter to evaluate relevance of multiscale model to reproduce the influence of compressive stress on the magnetostriction strain amplitude. Constants used for multiscale modelling are given in table 1.4. Figure 1.3c shows the <100> pole figure representative of the orientation data file used for modelling (170 orientations). Figures 1.7a-b-c-d allow experimental and modelling results to be compared, highlighting the ability of the multiscale strategy to model a complex reality (loading along the normal direction - orthogonal to (RD,TD) plane defined in pole figure).

«TABLE 4 HERE»

«FIGURE 7 HERE»

1.5 TWO RECENT EXTENSIONS OF THE MULTISCALE MODEL

Two extensions of the multiscale approach for magneto-mechanical behaviour are briefly discussed in this last section.

1.5.1 Second order magnetomechanical coupling for non-monotonic effects

It is not uncommon to observe for some materials that mechanical stress has a non-monotonic effect on magnetic behaviour. The non-monotonic effect concerns different iron-based ferromagnetic materials (iron-silicon, iron-cobalt, steels) when they are subjected to high stress level, though remaining far below the yield stress. Unlike the well-known Villari reversal, it may appear at the lowest magnetic field levels: it is for example characterized by a sudden decrease of initial susceptibility with increasing stress, although an increasing susceptibility is expected. This susceptibility variation change is accompanied by a magnetostriction variation change. Figure 1.8 illustrates that point for 29%Co-Fe lamination.

«FIGURE 8 HERE»

To address this non-monotony, a concept of demagnetising-stress can be introduced [14]. This theory does not explain however the associated apparent change of magnetostriction sign with stress. Micromagnetic models including magneto-elastic effects do not depict this phenomenon either. Indeed, most models use a formulation of free energy where the magneto-elastic coupling is linearly stress dependent. The definition of the mechanical part of the Gibbs free energy given by equation (1.29) is however not unique and corresponds to a first order Taylor expansion of a maybe more complex expression. The magneto-elastic part of Helmholtz free energy reads:

$$\psi_\alpha^{magmech} = -\mathbf{M}_\alpha \otimes \mathbf{M}_\alpha : \mathcal{E}_\alpha : \boldsymbol{\sigma}_\alpha = -M_s^2\, \mathbf{R}_\alpha : \mathcal{E}_\alpha : \boldsymbol{\sigma}_\alpha \tag{1.62}$$

Quantity $M_s^2\, \mathcal{E}_\alpha$ is the fourth order magnetostriction tensor, function of three independent constants in the case of cubic symmetry. This number reduces to two constants (i.e. λ_{100} and λ_{111}) considering the (usual) incompressibility condition. However a second order development in stress is theoretically possible, as recently proposed in [5], leading to the so-called *morphic effect*. Its practicle implementation remains however challenging since introducing this second-order term involves the identification of the terms of a sixth-rank tensor $\mathbb{E}_\alpha$ ($M_s^2\, \mathbb{E}_\alpha$ is the *morphic tensor*) following:

$$\psi_\alpha^{magmech} = -M_s^2\, \mathbf{R}_\alpha : (\mathcal{E}_\alpha : \boldsymbol{\sigma}_\alpha + \frac{1}{2}\boldsymbol{\sigma}_\alpha : \mathbb{E}_\alpha : \boldsymbol{\sigma}_\alpha) \tag{1.63}$$

The remaining scientific key points concern the development of a general method to obtain the magneto-elastic invariants whatever the crystallographic symmetry and generate functions of invariants required for an appropriate modelling of stress sensitivity of materials at high stress. NDE applications are particularly foreseen.

1.5.2 Magnetic shape memory alloys

Magnetic shape memory alloys (MSMA) are among the most promising alloys for designing miniature sensors or actuators. These materials are sometimes considered as *magnetostrictive* since magnetic field is also the source of their deformation. In these materials, the magnetisation process is the result of three competing mechanisms: the displacement of 180° magnetic domain walls and the local rotation of magnetisation vectors are the two usual sources of magnetostriction; the third and most significant phenomenon is the magnetic field induced variants reorientation. Indeed, in shape memory alloys, a high symmetry phase (austenite) stable at high temperature transforms into a lower symmetry phase (martensite) which can define different variants or twins (e.g. cubic austenite becomes quadratic martensite following three variants). In MSMA, each variant is constituted of antiparallel domains. Magnetization of such material occurs first by 180° magnetic domain walls in each variant. Then at a given magnetic field level, 90° magnetic domain walls displacement begins concomitant with twin walls. This mechanism leads to large deformation that may reach up to 12% in single crystals, and by consequence to a strong magnetoelastic coupling. The main interest of this mechanism is that it corresponds to a second order thermodynamic transformation that does not involve heat exchange. This is the reason why MSMA may be used at higher frequencies than other shape memory alloys (up to 1kHz).

A first attempt of multiscale modelling of these materials has been proposed in [15]. In this model, the variant scale ϕ (meaning martensite variant or the austenite phase) has been introduced between the grain g and domain α scales. According to the chemo-magneto-mechanical coupling and neglecting the boundary effects, the Gibbs free energy of a domain family must be complemented by the chemical energy $\mathfrak{g}_\alpha^T$ defined by:

$$\begin{aligned} \mathfrak{g}_\alpha^T &= h_\alpha - T s_\alpha \\ s_\alpha &= s_\alpha^0 + \rho_\alpha c_\alpha^p \left[1 - \frac{T^0}{T} + ln\left(\frac{T^0}{T}\right)\right] \end{aligned} \tag{1.64}$$

h_α and s_α are the enthalpy and entropy densities of the phase to which the domain α belongs. T indicates the temperature (considered as homogeneous). s_α^0 is the entropy density at reference temperature T^0. c_α^p is the specific heat and ρ_α the mass density. Results obtained by this modelling are encouraging.

1.6 CONCLUSION

Due to the complexity of the mechanisms involved, and to the strong nonlinearities of the behaviour, the modelling of magnetostrictive materials remains an open field of research. This section gives a brief overview of some key challenges to be addressed.

A first family of challenges lies in the wide variety of loadings to which magnetostrictive materials are subjected. The question of rotating magnetic fields for instance is not fully solved from the modelling point of view. Indeed, depending on the magnitude of the magnetic field, the activated mechanisms will appear in different proportions: at low induction level, a rotating field activates mostly domain wall motion, while magnetisation rotation is prominent for higher levels of magnetic field near saturation. This has consequences on the modelling strategies to be able to describe the different regimes. The multiaxiality is also a key question. Although the approach presented in this chapter is fully multiaxial, the validation process requires comparison to experimental data. Most of experimental apparatus for the characterisation of magneto-elastic behaviour are restricted to uniaxial tension or compression tests. Significant progress has been made in the past years to propose experimental equipment able to apply simultaneous magnetic field and multiaxial stress to magnetic materials. But in most cases, the tests performed on such equipment do not include magnetostriction strain measurements. Complementary validation experiments involving complex, representative loading configurations have to be imagined. Another point is the question of simultaneous stress and magnetic field variation, even in the quasi-static regime. This chapter has shown how hysteresis can be included in multiscale approaches. But the proposed methodology assumes that either stress or magnetic field are constant while the other loading quantity varies. No

multiscale modelling approach so far can describe the hysteretic response of a magnetostrictive material subjected to simultaneously varying stress and magnetic field.

The extension of multiscale modelling approaches in order to incorporate additional effects or specific configurations not included in the original approach is another family of challenges. Thermal effects for instance are often encountered when using magnetostrictive devices either because of harsh environment or because of self-heating issues. The introduction of a proportionality relationship between temperature and A_s parameter in equation (1.42) is consistent with the Boltzmann-like approach. However, the dependency of material parameters to temperature (saturation magnetisation, magnetostriction coefficients, elastic stiffness, etc) should also be incorporated in the constitutive equations. This extension to thermo-magneto-elastic behaviour is yet to be investigated through the multiscale approach. The forming and assembly processes lead to a very significant alteration of magneto-elastic properties. The multiscale approach seems a legitimate tool to address these issues assuming that the effect of processing is mainly expressed through residual stresses introduced in materials. The variety of processes used to shape magnetic materials makes it a wide field of investigation, although the main challenge probably lies in the modelling of the forming processes themselves. Another key parameter is time. Indeed, the properties of magnetostrictive materials often show some erosion with time. This degradation should be incorporated in the modelling since it alters the nominal performance of devices. This explains why ageing, also called functional fatigue (by opposition to mechanical fatigue eventually leading to fracture) are a dynamic topic of investigation in the field of smart materials. Finally the so-called *scale separation* assumption is sometimes to be questioned. Indeed, the multiscale approach relies on the idea that the different scales are well separated so that the behaviour can be averaged (homogenised) at each scale independently. This assumption is verified in most applications. But with the pressure of miniaturisation, it may not be fulfilled, for instance in magneto-electric micro and nano-devices. The case of strongly textured materials for which domains can cross grain boundaries and cover several grains is another example where the scale separation should be considered with caution.

The implementation of multiscale modelling approaches into numerical analysis software for the design of smart systems is another important challenge. Of course, calculation power keeps growing but, for engineering purposes, simplifications in the modelling procedure are a required path to exploit multiscale approaches. This question is addressed in the chapter "Multi-scale modelling of magnetic materials". An interesting area of application that requires intensive numerical modelling is non-destructive evaluation of stress using magnetic measurements (hysteresis loops, incremental permeability, eddy currents, or Barkhausen noise). A very promising technique relies on the combination

of acoustic and magnetic techniques for the assessment of internal stress using ElectroMagnetic Acoustic Transducers (EMAT). When applied to non-magnetic conductive materials the acoustic wave is generated by Lorentz forces, but when applied to magnetic materials, magnetostriction strain acts as a supplementary source to the elastic wave. The modelling of such an intricate phenomenon is a challenging task, both for the behaviour and numerical aspects.

Finally, it is worth noting that the approach proposed in this chapter is not strictly restricted to magnetostrictive materials but can be extended to a wider range of smart materials for which the macroscopic response is the result of a microstructure evolution. All ferroic materials (ferroelectric, ferromagnetic, ferroelastic) stand in this category. The case of magnetic shape memory alloys (MSMA) has been shortly discussed in the previous section. The multiscale strategy can also be particularly relevant for the multiscale modelling of magnetocaloric materials, which have properties very close to MSMA. Indeed, beyond magnetic refrigeration, high temperature magnetocaloric materials can be used as an active substance in thermomagnetic power conversion devices or wasted power harvesting systems. The strong magneto-elastic coupling in these alloys makes the role of microstructural features (local strains, coupling with surface and linear defects) as relevant as the intrinsic ones.

As a general conclusion, this chapter presented the main features of a multiscale approach for the modelling of magnetostrictive materials. Multiscale approaches can be in many applications a good trade-off between micromagnetic approaches, that often lead to prohibitive computation costs for the modelling of electromagnetic systems, and macroscopic phenomenological approaches, that ignore the microstructure of materials and often fail to capture the complex mechanisms of magneto-elastic interactions. A main advantage of multiscale approaches is that, in addition to providing a prediction of the macroscopic behaviour, they can shed a light on the relative influence of different mechanisms at play at the microstructural level.

ACKNOWLEDGEMENTS

In addition to the contributions by the authors, this chapter is largely based on the works of former and present PhD students R. Corcolle, N.Galopin, K.J. Rizzo, M. Rekik, S. Lazreg, A. Ouaddi. We are grateful for their contribution.

LIST OF FIGURES

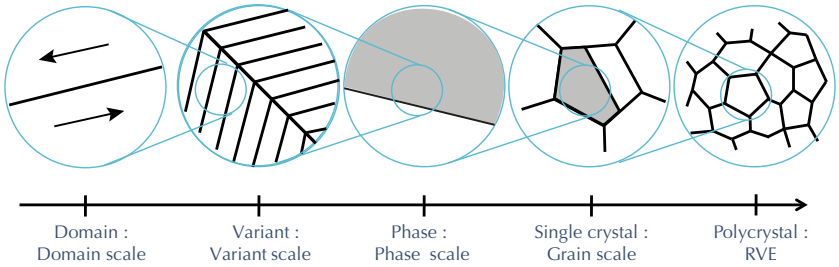

FIGURE 1.1 Scales involved in the modelling approach (arrows represent local magnetisation vectors).

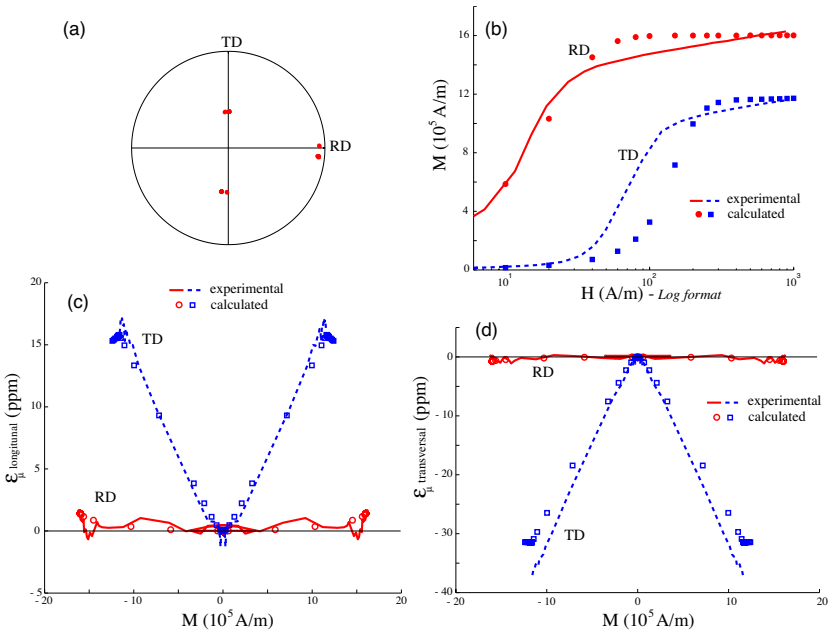

FIGURE 1.2 (a) <100> pole figure; Comparison between experimental (lines) and modelled (points) anhysteretic magnetisation (b), longitudinal (c) and transversal magnetostriction (d) along the rolling (RD) and transverse (TD) directions [10].

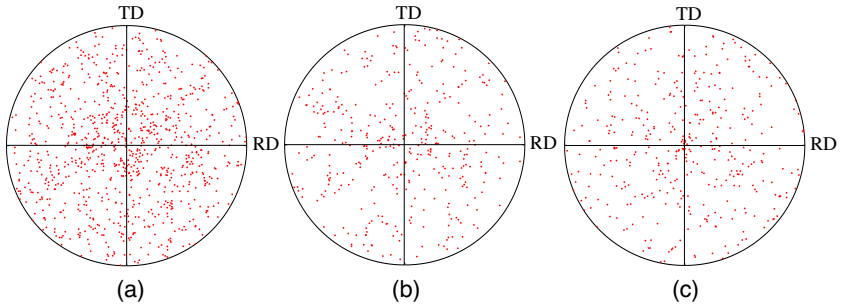

FIGURE 1.3 <100> pole figure used for multiscale modelling of: (a) low carbon steel - 299 orientations; (b) FeCo - 126 orientations; (c) Terfenol-D - 170 orientations.

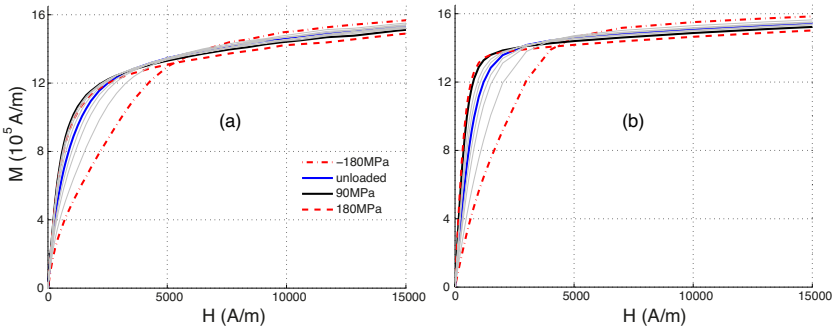

FIGURE 1.4 Comparison between experimental (a) and modelled (b) anhysteretic magnetisation of low carbon steel submitted to uniaxial stress (intermediate stress levels are depicted in grey lines).

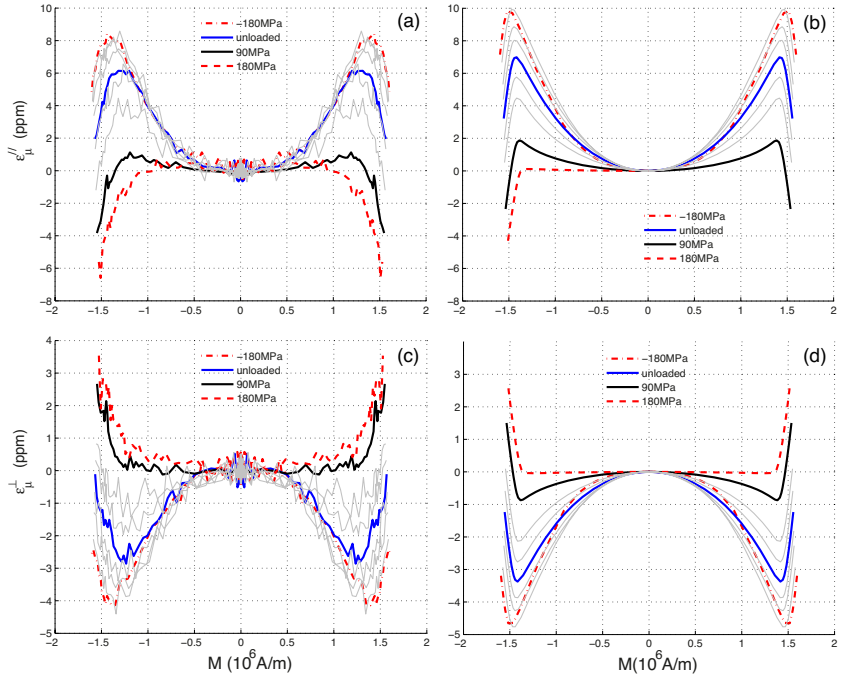

FIGURE 1.5 Comparison between experimental (a-c) and modelled (b-d) anhysteretic longitudinal (a-b) and transversal (c-d) magnetostriction of low carbon steel submitted to uniaxial stress (intermediate stress levels are depicted in grey lines).

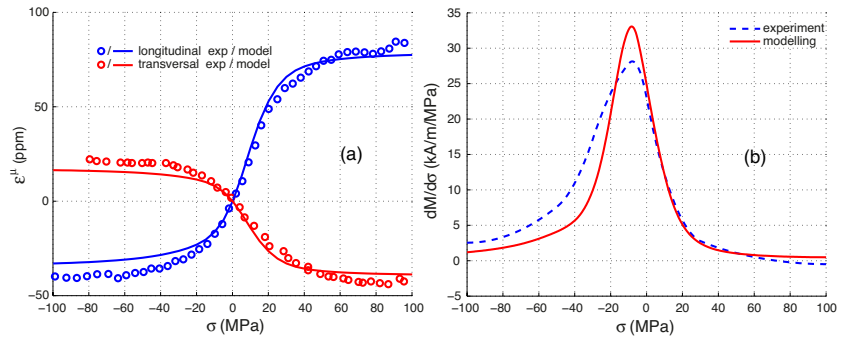

FIGURE 1.6 Comparison between experimental [12] and model for Fe-Co: (a) longitudinal and transversal magnetostriction as function of stress (H=0A/m) (ΔE effect); (b) Piezomagnetic sensitivity to stress at H=1000A/m.

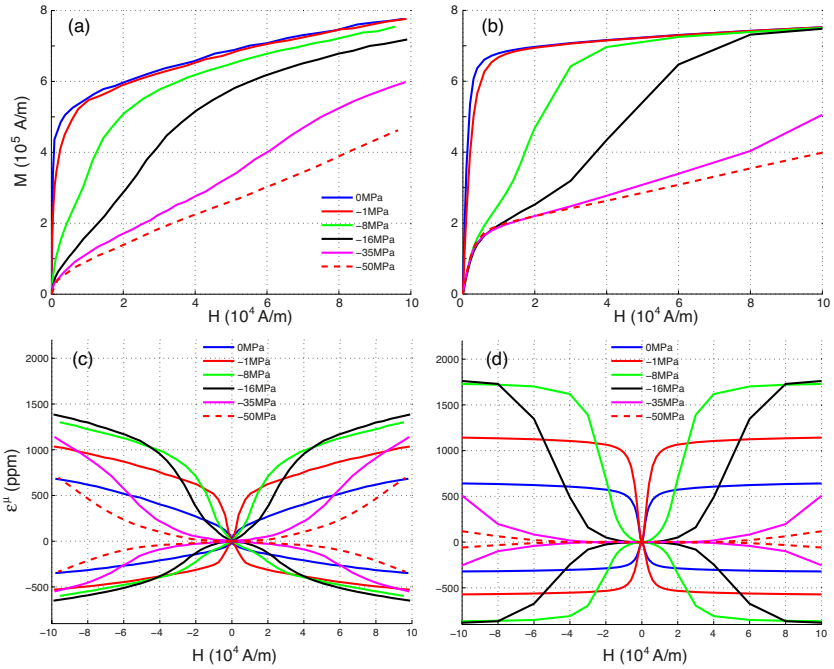

FIGURE 1.7 Comparison between experimental (a-c)[13] and modelling (b-d) for Terfenol-D under applied compressive stress: (a-b) magnetic behaviour; (c-d) longitudinal and transversal (negative) magnetostriction as function of stress.

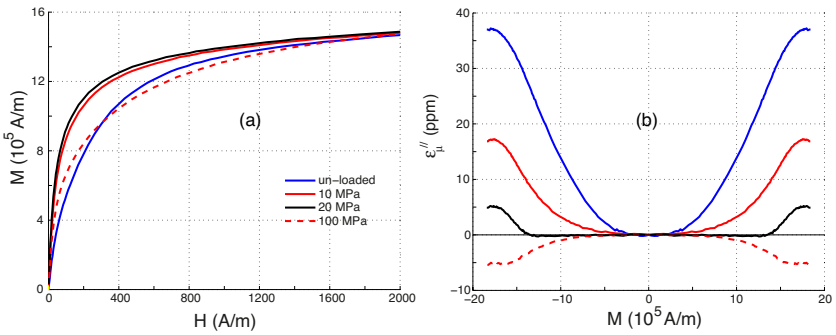

FIGURE 1.8 Magnetic (a) and longitudinal magnetostrictive (b) behaviour of 29%Co-Fe under applied stress. Illustration of non-monotonic effect - initial increasing (between 0 an 20MPa), then decreasing (above 20MPa) of magnetisation at given magnetic field; associated apparent change of magnetostriction sign above 20MPa.

LIST OF TABLES

TABLE 1.1 Physical constants used for the multiscale modelling of 3%Si-Fe electrical steel

coefficient	M_s	K_1 ; K_2	λ_{100} ; λ_{111}	A_s	C_{11} ; C_{12} ; C_{44}	N_s
unit	A/m	kJ.m^{-3}	ppm	m^3.J^{-1}	GPa	J.m^{-3}
value	1.61×10^6	38; 0	23 ; -4.5	2.0×10^{-2}	202 ; 122 ; 229	400

TABLE 1.2 Physical constants used for the multiscale modelling of low carbon steel

coefficient	M_s	K_1 ; K_2	λ_{100} ; λ_{111}	A_s	C_{11} ; C_{12} ; C_{44}	N_s
unit	A/m	kJ.m^{-3}	ppm	m^3.J^{-1}	GPa	J.m^{-3}
value	1.71×10^6	42; 15	21 ; -21	1.3×10^{-3}	238 ; 142 ; 232	0

TABLE 1.3 Physical constants used for the multiscale modelling of equiatomic iron-cobalt alloy - N_{RD} refers to configuration energy parameter along RD axis.

coefficient	M_s	K_1 ; K_2	λ_{100} ; λ_{111}	A_s	C_{11} ; C_{12} ; C_{44}	N_{RD}
unit	A/m	kJ.m^{-3}	ppm	m^3.J^{-1}	GPa	J.m^{-3}
value	1.89×10^6	35; 0	125 ; 30	1.5×10^{-3}	296 ; 153 ; 192	-340

TABLE 1.4 Physical constants used for the multiscale modelling of Terfenol-D

coefficient	M_s	K_1 ; K_2	λ_{100} ; λ_{111}	A_s	C_{11} ; C_{12} ; C_{44}	N_s
unit	A/m	kJ.m^{-3}	ppm	m^3.J^{-1}	GPa	J.m^{-3}
value	0.8×10^6	-80; -180	90 ; 1640	2×10^{-3}	141 ; 65 ; 49	0

NOMENCLATURE

RVE Representative Volume Element - polycrystal
g grain
ϕ phase
α domain scale or domain family
β domain family (index)
f_α domain family volume fraction
$\theta_\alpha, \phi_\alpha$ spherical angles associated with a domain family α

e_α^c kinetic energy density (J.m^{-3})
u_α internal energy density (J.m^{-3})
ψ_α Helmholtz free energy density (J.m^{-3})
ψ_α^μ magnetomechanical part of the Helmholtz free energy density (J.m^{-3})
s_α entropy density (J.K^{-1}.m^{-3})
h_α enthalpy density (J.m^{-3})
$\mathfrak{g}_\alpha$ Gibbs free energy (free enthalpy) density (J.m^{-3})
$\mathfrak{g}_\alpha^{mech}$ mechanical part of the Gibbs free energy density (J.m^{-3})
$\mathfrak{g}_\alpha^{mag}$ magnetic part of the Gibbs free energy density (J.m^{-3})
$\mathfrak{g}_\alpha^\mu$ magnetomechanical part of the Gibbs free energy density (J.m^{-3})
$\mathfrak{g}_\alpha^S$ surface (demagnetising) effect part of the Gibbs free energy density (J.m^{-3})
$\mathfrak{g}_\alpha^T$ chemical part of the Gibbs free energy density (J.m^{-3})
p_α total mechanical power density (W.m^{-3})
p_α^e electromagnetic power density (W.m^{-3})
p_α^m mechanical power density (W.m^{-3})

q_α local heat source (W.m^{-3})
$\mathbf{q}_\alpha^s$ local heat transfer (W.m^{-2})
T_α local temperature (K)
T temperature at the RVE scale (K)
$\mathbf{v}_\alpha$ local velocity (m.s^{-1})
$\mathbf{\Gamma}_\alpha$ local acceleration (m.s^{-2})
$\mathbf{f}_\alpha$ body forces (N.m^{-3})
$\mathbf{f}_\alpha^{em}$ electromagnetic body forces (N.m^{-3})
$\boldsymbol{\sigma}_\alpha$ local Cauchy stress tensor (N.m^{-2})
$\boldsymbol{\sigma}_\alpha^{rev}$ reversible part of the local Cauchy stress tensor (N.m^{-2})
$\boldsymbol{\sigma}_\alpha^{irr}$ irreversible part of the local Cauchy stress tensor (N.m^{-2})
$\boldsymbol{\sigma}_\alpha^M$ local Maxwell stress tensor (N.m^{-2})
$\boldsymbol{\sigma}_g$ stress tensor at the grain scale (N.m^{-2})
$\boldsymbol{\sigma}$ stress tensor at the RVE scale (N.m^{-2})
σ stress (scalar) (N.m^{-2})
σ_{rev} reversible stress (scalar) (N.m^{-2})
σ_{irr} irreversible stress (scalar) (N.m^{-2})

$\boldsymbol{\epsilon}_\alpha$ linearised strain tensor
$\boldsymbol{\epsilon}_\alpha^e$ elastic strain tensor
$\boldsymbol{\epsilon}_\alpha^\mu$ local magnetostriction strain tensor
$\boldsymbol{\epsilon}_\alpha^{\mu-rev}$ reversible part of local magnetostriction strain tensor
$\boldsymbol{\epsilon}_\alpha^{\mu-irr}$ irreversible part of local magnetostriction strain tensor
$\boldsymbol{\epsilon}_g^\mu$ magnetostriction strain tensor at the grain scale
$\boldsymbol{\epsilon}^\mu$ magnetostriction strain tensor at the RVE scale
ϵ^μ magnetostriction strain (scalar)
ϵ_{prev}^μ previous magnetostriction strain (scalar)

$\mathbf{J}_\alpha$ local current density (A.m^{-2})
$\mathbf{E}_\alpha$ local electrical field (V.m^{-1})
$\mathbf{H}_\alpha$ local magnetic field (A.m^{-1})
$\mathbf{H}_\alpha^d$ local demagnetising field (A.m^{-1})
$\mathbf{H}_g$ magnetic field at the grain scale (A.m^{-1})
$\mathbf{H}$ magnetic field at the RVE scale (A.m^{-1})
$\mathbf{H}_\alpha^{rev}$ reversible part of local magnetic field (A.m^{-1})
$\mathbf{H}_\alpha^{irr}$ irreversible part of local magnetic field (A.m^{-1})
H magnetic field (scalar) (A.m^{-1})
H_{rev} reversible magnetic field (scalar) (A.m^{-1})
H_{irr} irreversible magnetic field (scalar) (A.m^{-1})
$\mathbf{J}'_\alpha$ local convective current density (A.m^{-2})
$\mathbf{E}'_\alpha$ local convective electrical field (V.m^{-1})
$\mathbf{H}'_\alpha$ local convective magnetic field (A.m^{-1})
$\mathbf{D}_\alpha$ local electrical displacement (A.s.m^{-2})
$\mathbf{B}_\alpha$ local magnetic induction (V.s.m^{-2})
$\mathbf{M}_\alpha$ local magnetisation (A.m^{-1})
M_α local magnetisation (scalar) (A.m^{-1})
$\mathbf{M}_g$ magnetisation at the grain scale (A.m^{-1})
$\mathbf{M}$ magnetisation at the RVE scale (A.m^{-1})
M magnetisation (scalar) (A.m^{-1})
M_{prev} previous magnetisation (scalar) (A.m^{-1})
$\mathbf{M}_\alpha^{rev}$ reversible part of local magnetisation (A.m^{-1})
$\mathbf{M}_\alpha^{irr}$ irreversible part of local magnetisation (A.m^{-1})

ρ_α mass density (kg.m^{-3})
ρ_α^e electrical charge density (C.m^{-3})
C_α local stiffness tensor (GPa)
C_{ij} stiffness constants - Voigt notation (GPa)
μ_0 vaccuum magnetic permeability (= $4\pi\times10^{-7}$Henry.m^{-1})
M_s saturation magnetisation (A.m^{-1})
A magnetic exchange constant (J.m^{-1})
$\mathbf{K}_\alpha$ second rank magnetocrystalline tensor (s.i.u.)
$\mathcal{K}_\alpha$ fourth rank magnetocrystalline tensor (s.i.u.)

$\mathbb{K}_\alpha$ sixth rank magnetocrystalline tensor (s.i.u.)
K_0, K_1, K_2 magnetocrystalline constants (J.m^{-3})
$\mathcal{E}_\alpha$ fourth rank magnetostriction tensor (s.i.u.)
$\mathbb{E}_\alpha$ sixth rank magnetostriction (morphic) tensor (s.i.u.)
λ_{100}, λ_{111} magnetostriction constants
χ_0 initial susceptibility
χ_m secant susceptibility at the RVE scale
$\mathcal{B}_g$ stress concentration tensor
C^{acc} accomodation stiffness tensor (GPa)
N_s demagnetising field factor
C surface effect constants (J.m^{-3})
C_0 surface effect factor
K_c configuration energy constant (J.m^{-3})
c_α^p specific heat capacity (W.kg^{-1}.K^{-1})
H_C coercive magnetic field (A.m^{-1})
a', k_a,κ, κ_0 parameters for magnetic hysteresis
σ_C coercive stress (N.m^{-2})
a', k'_a, κ', κ'_0 parameters for piezomagnetic hysteresis
T^0 reference temperature (K)
s_α^0 reference local entropy (J.K$^-$1.m^{-3})

$\boldsymbol{\alpha}$ direction of magnetic domain family α
α_i (i=1,2,3) direction cosine of magnetic domain family α
$\mathbf{e}_i$ (i=1,2,3) crystal frame
$\mathbf{R}_\alpha$ second rank orientation tensor
$\mathbf{N}$ demagnetising tensor
$\mathbf{Q}$ configuration matrix
$\mathbf{z}_0$ unit vector normal to the sheet plane
δ sign parameter ($\pm$ 1)

$\dot{[\,]}$ partial time derivative
${}^t[\,]$ transpose
. scalar product
$\otimes$ tensorial product
$\wedge$ vectorial product
: second order contraction
$\|...\|$ norm of a vector

Bibliography

[1] R. M. Bozorth, "Ferromagnetism", ed. Van Norstand Company, Berlin, New York, 1951.

[2] B.D. Cullity, "Introduction to Magnetic Materials", Addison-Wesley, Reading MA, 1972.

[3] A.C. Eringen and G.A. Maugin, "Electrodynamics of continua I - foundations and solid media", ed. Springer-Verlag, New York, 1990.

[4] J. Lemaitre, J.L. Chaboche, A. Benallal and R. Desmorat, "Mécanique des matériaux solides", 3rd edition, ed. Dunod, 2009.

[5] O. Hubert, "Multiscale magneto-elastic modeling of magnetic materials including isotropic second order stress effect", *Journal of Magnetism and Magnetic Materials*, **491**, (2019), 1-16, 165564.

[6] G. Bertotti, "Hysteresis in Magnetism: For Physicists, Materials Scientists, and Engineers", ed. Academic Press, San Diego, New York, 1998.

[7] N. Buiron, L. Hirsinger and R. Billardon, "A multiscale model for magneto-elastic couplings", *Journal de Physique IV*, **9** (1999), pp.187-196.

[8] L. Daniel, O. Hubert, N. Buiron and R. Billardon, "Reversible magneto-elastic behavior: a multiscale approach", *Journal of the Mechanics and Physics of Solids*, **56** (2008), pp.1018-1042.

[9] O. Hubert, S. Lazreg, "Two phase modeling of the influence of plastic strain on the magnetic and magnetostrictive behaviors of ferromagnetic materials", *Journal of Magnetism and Magnetic Materials*, **424** 2 (2017), pp.421-442.

[10] O. Hubert, L. Daniel, "Multiscale modelling of magneto-mechanical behaviour of Grain Oriented Silicon Steels", *Journal of Magnetism and Magnetic Materials*, **320**, (2008), pp.1412-1422.

[11] H. Hauser, "Energetic model of ferromagnetic hysteresis: Isotropic magnetization", *Journal of Applied Physics*, **96** 5, (2004), 2753-2767.

[12] O.Hubert, R.Waberi, S.Lazreg, H.S.Kim and R.Billardon, "Measurement and two-scales modeling of the ΔE effect", 7th European Solid Conference - ESMC 2009, Lisbonne, Portugal (2009).

[13] M. Domenjoud, E. Berthelot, N. Galopin, R. Corcolle, Y. Bernard, L. Daniel, "Characterization of Giant Magnetostrictive Materials under static stress : influence of loading boundary conditions", *Smart Materials and Structures*, **28**(9) (2019) 095012.

[14] C. Schneider, "Effect of stress on the shape of ferromagnetic hysteresis loops", *Journal of Applied Physics*, **97** (2005), 10E503.

[15] M.D. Fall, O.Hubert, F. Mazaleyrat, K. Lavernhe-Taillard and A. Pasko, "Multiscale Modeling of Magnetic Shape Memory Alloys: Application to NiMnGa Single Crystal", *IEEE Transactions on Magnetics*, **52** 5 (2016), pp.1-4.